

Electrochemical Migration Failure of the Copper Trace on Printed Circuit Board Driven by Immersion Silver Finish

Yilin Zhou*, Pan Yang, Chengming Yuan, Yujia Huo

Beijing University of Posts and Telecommunications, Internal box 71, 10 Xitucheng Road, Haidian District, Beijing 100876, P. R. China
yizhou@bupt.edu.cn

With lead-free legislation impacting printed circuit board (PCB) manufacturing, immersion silver (ImAg) finish is adapted as the top finish of copper trace on PCB due to its many advantages. However, it is easy for silver to form electrochemical migration (ECM) in high humid environment, so that the potential bias and spacing between adjacent circuits are limited. In addition, since the thickness of ImAg finish is usually less than 0.15 μm restrained by the electroless plating process, the copper trace under the silver finish cannot be fully covered, which causes the complexity of corrosion and electrochemical migration. In this paper, water drop test was used to induce the electrochemical migration on ImAg finished "Y" pattern circuits on PCB. The surface insulation resistance was detected by a picoammeter and the growth of dendrite deposit between two electrodes was monitored by a video system. The electrolytic reaction and galvanic reaction on the electrodes formed by bimetal couples was analyzed theoretically. The mechanism of electrochemical migration of copper driven by immersion silver finish was discussed. The effects of potential bias, spacing and electric field intensity between adjacent circuits on electrochemical migration were discussed.

1. Introduction

Surface finishes are commonly used to protect the copper metallization of a PCB from oxidation to enable good solderability of the PCB. With lead-free legislation impacting PCB manufacturing on a global scale, the ImAg finish is rapidly gaining popularity as the lead-free surface finish of choice, described by Ganesan and Pecht (2006). ImAg serves as a protective finish, thereby ensuring the solderability of the underlying copper on PCB for up to 12 months prior to assembly, which was studied by Vianco (1998), Lopez et al. (2005), and Filip et al. (2002). However, silver migration has been reported by Kohman since 1955. Under the influence of a direct current bias, silver ions move from anode to cathode through the adsorbed water layer on the insulation surface to form dendrites. As a result, the surface insulation resistance (SIR) decreases significantly, which is called ECM and discussed by Steppan, et al. (1987) and Krumbein (1988). The ECM processes usually involve several steps: water adsorption, anodic metal dissolution or ion generation, ion accumulation, ion migration to cathode, and metal dendritic growth, reported by Yang et al. (2006). The time to failure (TTF) models estimate the time for dendritic growth between adjacent conductors, not only involving ion generation, ion transport, and metal deposition, but also considering temperature, humidity, bias, ion concentration and current density effects reported by DiGiacomo (1982) Bhakta et al. (2002), Jung et al. (2003) and Peck (1986). The TTF model was even revised to predict the time for surface insulation resistance degradation caused by ion accumulation prior to the dendritic growth between adjacent conductors by Yang and Christou (2007). ECM of many kinds of metals using in electric packaging were compared, such as Ag, Sn, Pb, Cu and so on, by DiGiacomo (1982) and Nohm et al. (2009).

In this paper, the ECM failure of the ImAg finished copper trace on PCB was studied by water drop test. The galvanic reaction and electrolytic reaction occurred on the electrodes, which are formed by bimetal couples, were analyzed. The effects of potential bias, spacing and electric field intensity between adjacent circuits on ECM of copper trace were also assessed by experimental simulation.

2. Experimental methods

Water drop test is adopted as an accelerated experiment to analyze the ECM of ImAg finished PCB.

2.1 Experimental samples

According to IPC-TM-650 "test methods manual" to assess the susceptibility to metallic dendritic growth of uncoated printed wiring, the test PCB was designed as "Y" pattern with a pair of paralleled conductors having 0.318 mm, 0.450 mm and 0.635 mm spacing respectively, shown in Figure 1. The thickness of ImAg finish is about 0.15 μm .

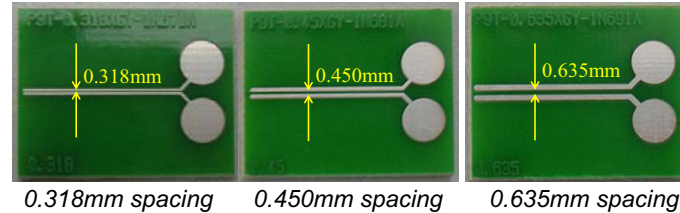


Figure1: Test PCB with "Y" pattern paralleled conductors

2.2 Experimental devices

A measurement system for water drop tests was designed, shown in Figure 2. The test system is consisted of a SIR measurement unit, a video monitor unit and an anti-interference unit. In the SIR measurement unit, the 5-digit Model 6487 Picoammeter was adopted to measure the SIR between "Y" pattern conductors during water drop tests about every 60 ms. A 10 k Ω resistor was connected with the conductor of positive electrode in series to protect from the short circuit once the dendrites grew. In the video monitor unit, an optical microscope was used to observe the ECM phenomenon in water drop and to input the visual record to PC. In the anti-interference unit, a triaxial cable and a twisted pair wire were applied to connect the picoammeter and the tested PCB in a shielding box so as to reduce interference. A deionized water machine is used to supply pure water, whose resistivity is 18.2 M $\Omega\cdot\text{cm}$.

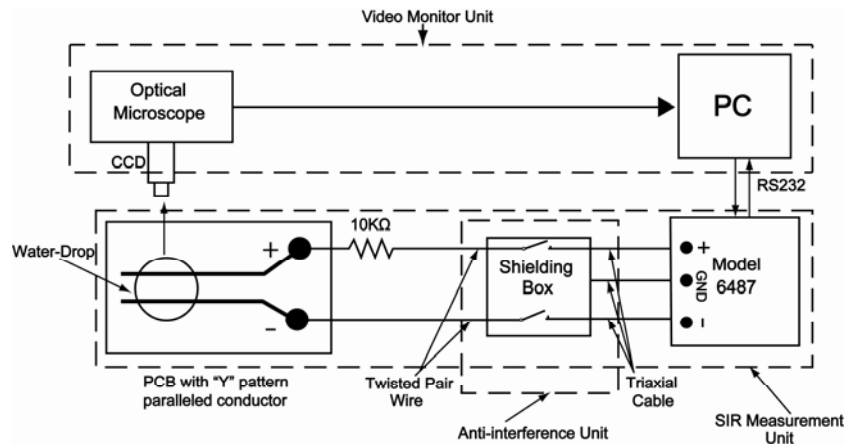


Figure 2: The system block diagram for water drop tests

2.3 Experimental matrix

The potential bias and the spacing between two paralleled conductors will have strong impacts on the growth of dendrites based on the ECM mechanism. Four potential bias (1.5V, 2V, 3V, 5V) and three spacing (0.318 mm, 0.450 mm, 0.635 mm) were selected. Five experiments were repeated under every test conditions.

3. Experimental results

3.1 The formation process of dendrites and change of SIR

The test result of Y pattern PCB with 0.450 mm spacing under 5V potential bias was taken as a typical example, whose SIR curve is shown in Figure 3. The phenomenon of ECM in various stages were taken photos, shown in Figure 4a~d respectively.

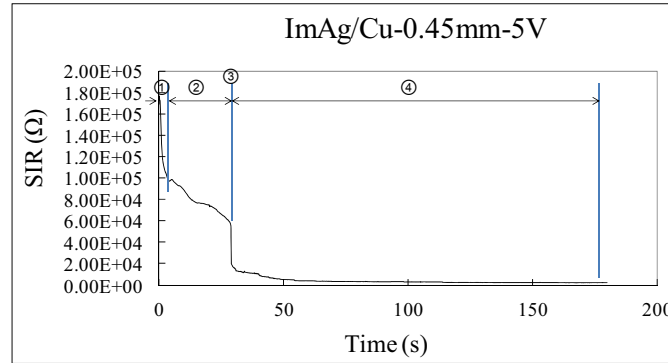


Figure 3: SIR of Y pattern PCB with 0.450 mm spacing under 5.0 V potential bias in water drop test

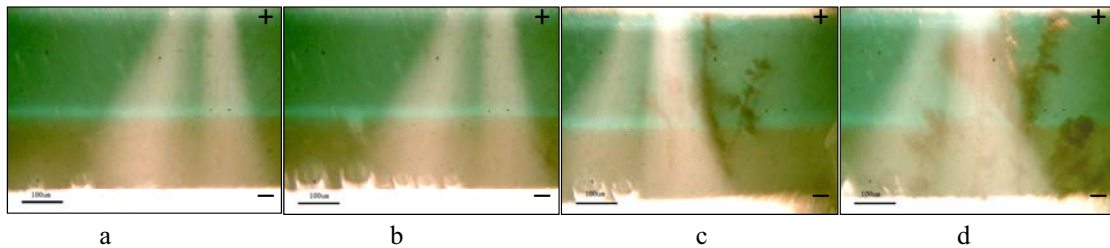


Figure 4: The phenomenon of ECM happened on Y pattern PCB with 0.450 mm spacing under 5.0 V potential bias in water drop test

Combining the SIR curve and the formation of dendrites, it could deduce that the ECM progress was consisted of two stages, a gestation stage and a conductive deposits growth stage.

The first stage can be divided into two steps according to the SIR curve in Figure 3. The step 1 started from the very beginning and lasted for about 3.64 s. Once the potential bias was input on the adjacent paralleled conductors on Y pattern PCB, the SIR dropped from 176 K Ω to 100 k Ω immediately. A few bubbles appeared along the negative electrode, as shown in Figure 4a. After that, SIR decreased gradually to 59 k Ω in 25.14 s of the step 2, and many bubbles were produced along the cathode, corresponding to the Figure 4b. Based on the observation of various test results, it was found that the higher the potential bias was, the quicker the bubbles were produced.

The second stage followed the first one. In this stage, the conductive deposits with dendrite shape grew to cause the serious drop of SIR. According to the SIR curve and the formation process of dendrites, this stage could also be divided into two steps further. The step 3 happened from 28.78 s to 29.09 s, the step 4 followed and lasted until the end. In the step 3, one main dendrite quickly formed to short circuits, as shown in Figure 4c, which caused SIR curve to drop from 59 K Ω to 19.87 K Ω in 0.31 s. The growth of dendrite almost happened in one moment, like seaweed surfaced from water. As the potential bias reduced, it could be observed that the dendritic deposits grew from cathode to anode. In the step 4, the multiple dendrites gradually formed and grew from cathode to anode slowly accompanying with the main dendrite in the step 3, which reduced the SIR further to 2 K Ω in 3 min. Some of them can reach to the anode, the others just stop between two electrodes, as shown in Figure 4d.

3.2 The element compositions of the dendrites

The morphology of the dendrites formed in water drop test was observed by environmental scanning electronic microscope (ESEM), shown in the Figure 5. The element compositions on the dendrites were detected by X-ray dispersive energy microscope (XEDS), the atomic percentage of Ag and Cu was listed in Table 1. It was seen that the atomic percentage of Cu was about 3.5 times of that of Ag on the light grey

migration products close to the cathode, like point 1 in Figure 5, but the atomic percentage of Cu was about 16 times of that of Ag on the dark grey migration products close to anode, like point 2 in Figure 5. Cu even migrated and deposited on the surface of cathode, as point 3 in Figure 5.

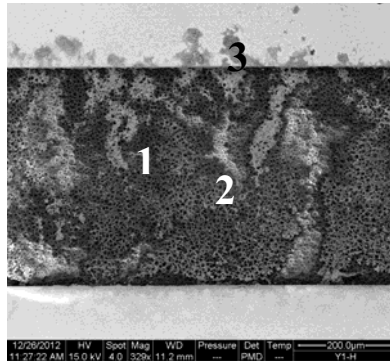


Figure 5: The dendrites between Y pattern paralleled circuits formed in water drop test

Table 1: Contents of Ag and Cu (atomic percentage) on the migration products

| | Ag | Cu |
|---------|---------|---------|
| Point 1 | 21.99 % | 78.01 % |
| Point 2 | 5.89 % | 94.11 % |
| Point 3 | 4.42 % | 95.58 % |

3.3 Influencing factors on electrochemical migration

The SIR of 50 kΩ was taken as a criteria. The time it took for the SIR to reduce to 50 kΩ was picked up in water drop tests as the time to failure (TTF). Then Weibull distribution was used to calculate the characteristic TTF of five repeated tests at the confidence level 98 % for each test condition, which was recorded in Table 2.

Table 2: Characteristic TTF of Y pattern PCB in water drop tests

| Spacing(mm) | Bias (V) | | | | |
|-------------|----------|-------|-------|------|--|
| | 1.5 | 2 | 3 | 5 | |
| 0.318 | 308.6 | 107.0 | 37.2 | 7.7 | |
| 0.450 | 623.9 | 203.5 | 118.0 | 26.5 | |
| 0.635 | 1108.8 | 282.0 | 172.4 | 47.3 | |

According to Table 2, the fitting curves of the characteristic TTF vs. electric field intensity (E) are drawn in Figure 6. The fitting function is power function, whose index of power function is -2.466. As the E increased, the TTF of PCB decreased quickly. However, when the E was same, for example, 1.5 V potential bias and 0.318 mm spacing forms same E with 3 V potential bias and 0.635mm spacing, the TTF was totally different, which were 308.57 s and 172.38 s respectively. This result means the potential bias has more contribution to the TTF than spacing.

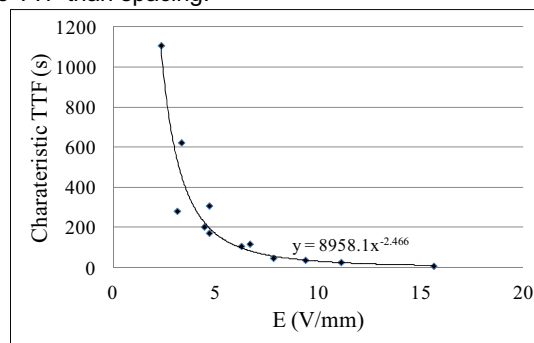


Figure 6: the fitting curve of the characteristics TTF vs E

4. Discussion

4.1 Mechanism of electrochemical migration

In this research, when the deionized water was dropped on the paralleled electrodes and the potential bias was input, an electrolytic cell reaction started immediately between two electrodes. Water was ionized to form H^+ and OH^- . The moving of both H^+ and OH^- driven by the potential bias caused the SIR dropped suddenly, corresponding to the step 1 in Figure 3. H^+ moved toward the negative electrode to gain electrons and form H_2 bubbles, and OH^- moved toward the positive electrode at the same time, so that the solution near the positive electrode appeared weakly alkaline environment.

Since the thickness of ImAg was only 0.15 μm , the copper substrate was possibly exposed from the pores and defects on the ImAg finish, especially from the sides of the circuits. Therefore, Ag and Cu formed a galvanic cell in the weakly alkaline environment around the anode. Since the standard electrode potential of Ag is +0.8 V, but that of Cu is +0.337, the electromotive force between Ag-Cu galvanic cell is 0.463 V. Anode Cu will lose electrons to form cation and dissolve in the water. Oxygen-absorbed corrosion happened on the Ag cathode. Once Cu^{2+} formed on the positive electrode, they will be attracted by the negative electrode, which reduce the concentration of Cu^{2+} around positive electrode to promote galvanic corrosion continued. The concentration of ions in the water drop increased, which caused SIR gradually reduced, appeared as in the step 2 in Figure 3. Until now, dendritic growth had not happened yet, so that this process was called a gestation period.

Then, Cu^{2+} will move to the negative electrode and get electrons to form first Cu deposit. Electrons went through Cu deposit to realize the reduction of following Cu^{2+} . Therefore, the dendrite like deposits seemed to grow from negative electrode. The velocity of the electrons transferred from the produced Cu deposits was higher than that of the ion motion in water, so the first dendrite bridging the paralleled electrodes seemed to form instantaneously, only 0.31s, and the SIR dropped sharply as shown in the step 3 in Figure 3. After that, Cu^{2+} from other exposed copper trace continued to migrate from positive electrode to negative electrode and form dendrites. But the potential bias between the electrodes had been reduced by primarily deposited dendrites, so the formation of dendrites became slower.

The galvanic corrosion on positive electrode pushed copper to lose electrons and protected silver, but a little part of Ag from the top finish was still hydrated and dissolved into water to form Ag^+ . Ag^+ and OH^- deposited as AgOH on the side of positive electrode. Then Ag_2O decomposed from AgOH was dispersed for colloid. After that, a hydrate reaction caused the Ag_2O to form AgOH again. As the reaction was advanced, silver ion moved to the negative electrode and formed dendritic deposition with copper, as point 1 in Figure 5. But as the Ag migrated, the exposed Cu on the positive electrode expanded, so more and more Cu migrated, the ratio of Cu and Ag on the deposits near positive electrode was 16:1, as point 2 in Figure 5. The electrochemical reactions happened on both electrodes were listed in Table 3. Therefore, the bimetal couple on the electrodes changed the order of metals tending to form electrochemical migration.

Table 3: Electrochemical reactions on the electrodes

| Positive electrode | Reaction Types | Negative electrode | Reaction Types |
|---|------------------------------------|---------------------------------|-------------------|
| $H_2O \rightarrow H^+ + OH^-$ | Electrolytic cell | $2H^+ + 2e^- \rightarrow H_2$ | Electrolytic cell |
| Anode: $Cu \rightarrow Cu^{2+} + 2e^-$ Cathode: $2H_2O + O_2 + 4e^- = 4OH^-$ | Oxygen-absorbed galvanic corrosion | $Cu^{2+} + 2e^- \rightarrow Cu$ | Electrolytic cell |
| $Ag \rightarrow Ag^+ + e^-$ $2AgOH = Ag_2O + H_2O$ $Ag_2O + H_2O = 2AgOH = 2Ag^+ + 2OH^-$ | Electrolytic cell | $Ag^+ + e^- \rightarrow Ag$ | Electrolytic cell |

4.2 Influencing factors on ECM

Taken the 50 K Ω as the criteria, the TTF of PCB failed by ECM appeared as a power function as E increased, whose index of power function is -2.466. The key steps of ECM were ion generation and ion migration, which decided the TTF. The velocity of ion migration is depended on the E, but the ion generation and number of charges is proportional to the potential bias analyzed by Yang (2007). Therefore, when the E was same, the TTF of higher potential bias and larger spacing is much shorter than that of lower potential bias and smaller spacing, which means the potential bias has more contribution to the TTF than spacing.

5. Conclusion

By water drop test, the electrochemical migration of ImAg finished copper trace on PCB was studied. Combining the SIR curve, the formation process of dendritic growth and element analysis, it could deduct that the ECM progress could be consisted of two stages, which were a gestation period and a conductive deposits growth stage. In the gestation period, an electrolytic reaction ionized water to form H^+ and OH^- , so the SIR dropped suddenly. Then the reduction of H^+ on negative electrode formed H_2 bubbles. An oxygen-absorbed galvanic corrosion happened on the positive electrode driven by the different standard electrode potential between Ag and Cu. Exposed Cu lost electrons to form cation. But a little part of Ag on the positive electrode was still hydrated to form Ag^+ and dissolved in the water. As the ion generation and accumulation, the SIR gradually reduced. In the conductive deposits growth stage, Cu^{2+} and Ag^+ formed on the positive electrode was attracted to move toward the negative electrode and gained electrons to produce primary Cu and Ag deposits, through which electrons were provided for following Cu^{2+} and Ag^+ arrived and caused SIR to drop sharply. Then, the dendrite like deposits grew from negative electrode to positive electrode until shorting.

The bimetal couple on the electrodes changed the order of metals tending to form electrochemical migration. Both Ag and Cu migrated from negative electrode to positive electrode, but the content of Ag was much lower than that of Cu in dendrites grown between ImAg finished electrodes.

The TTF of PCB failed by ECM appeared as a power function as electric field intensity increased, whose index of power function was -2.466. The potential bias has more contribution to the TTF than spacing because the ion generation and number of charges were proportional to the potential bias.

Acknowledge

The authors appreciate the Chinese Universities Scientific Fund to support this study.

References

- Bhakta S. D, Lundberg S, Mortensen G, 2002, Accelerated Tests to Simulate Metal Migration in Hybrid Circuits, in Proc. IEEE Annual Reliability and Maintainability Symposium, Seattle, WA, USA, 319–324.
- DiGiacomo G., 1982, Metal migration (Ag, Cu, Pb) in encapsulated modules and time-to-fail model as a function of the environment and package properties, Proc. IEEE 20th Int. Rel. Phys. Symp., San Diego, CA, 27–33.
- Filip Granit N., Korin E., Bettelheim A., 2002, Effect of Organic Additives on Electrochemical Surface Precipitation and Polymorphism of $CaCO_3$, Chemical Engineering Transactions, 1, 743-748.
- Ganesan S. Pecht M., 2006, Lead-Free Electronics, John Wiley and Sons, Inc., New York, USA.
- Jung J. S., Kim J. W., Kim M. S., Jang J. S., Ryu D. S., 2003, Reliability evaluation and failure analysis for NTC thermistor, Int. J. Mod. Phys. B, 17(8/9), 1254–1260.
- Kohman G. T., Hermance H. W., Downes G. H., 1955, Silver migration in electrical insulation, Bell Syst. Tech. J., 34(6), 1115–1147.
- Krumbein S. J., 1988, Metallic electromigration phenomena, IEEE Trans. Compon., Hybrids, Manuf. Technol., 11(1), 5–15.
- Lopez E., Vianco P., Buttry R., Lucero S., Rejent J., 2005, Effect of Storage Environments on the Solderability of Immersion Silver Board Finishes with Pb-Based and Pb-Free Solders, SMTA Journal, 18(4), 19-28.
- Noh B. I., Yoon J. W., Hong W. S., Jung S. B., 2009, Evaluation of Electrochemical Migration on Flexible Printed Circuit Boards with Different Surface Finishes, Journal of Electronic Materials, vol.38, No.6, 902-907, DOI:10.1007/s11664-009-0737-z.
- Peck D. S, 1986, Comprehensive model for humidity testing correlation, Proc. IEEE 24th Int. Rel. Phys. Symp., Anaheim, CA, 44–50.
- Steppan J. J., Roth J. A., Hall L. C., Jeannotte D. A., Carbone S. P., 1987, A Review of Corrosion Failure Mechanisms during Accelerated Tests, J. Electrochem. Soc.: Solid-State Sci. Technol., 134(1), 175–190.
- Vianco P., 1998, An Overview of Surface Finishes and Their Role in Printed Circuit Board Solderability and Solder Joint Performance, Circuit World, 25(1), 6-24.
- Yang S., Wu J., Christou A., 2006, Initial Stage of Silver Electrochemical Migration Degradation, Microelectronics Reliability, 46(9), 1915-1921, DOI:10.1016/j.microrel.2006.07.080.
- Yang S., Christou A., 2007, Failure Model for Silver Electrochemical Migration, IEEE Transactions on Device and Materials Reliability, 7(1),188-196, DOI:10.1109/TDMR. 2006.891531.